Zagazig University Medical Journal
www.zumj.journals.ekb.eg
https://doi.org/10.21608/zumj.2024.333297.3674 Volume 31, Issue ٢, FEB. 2025, Supplement Issue
Manuscript ID ZUMJ-2411-3674
DOI 10.21608/zumj.2024.333297.3674
ORIGINAL ARTICLE

Colchicine Alleviates Steroid-Induced Hyperglycemia and Dyslipidemia: Targeting Pyroptosis and Oxidative Stress

Mahitab M. Nageeb[1*], Samar Mortada Mahmoud[2], Shimaa Ali Mohamed Ali[3], Nihal Ibrahim hendy awadallah[4], Marwa M. Ahmad5, Dalia A. Hemead[4]
[1] Pharmacology Department, Faculty of Medicine, Zagazig University, Zagazig, Egypt
[2] Anatomy and Embryology Department, Faculty of Medicine, Zagazig University, Zagazig , Egypt
[3] Biochemistry Department, Faculty of Medicine, Al-Azhar University, Cairo, Egypt
[4] Physiology Department, Faculty of Medicine, Zagazig University, Zagazig, Egypt

***Corresponding author:**
Mahitab M. Nageeb

e-mail: MMAbdulWahab @medicine.zu.edu.eg

Submit Date 06-11-2024
Revise Date 25-11-2024
Accept Date 04-12-2024

ABSTRACT

Background Steroid-induced hyperglycemia (SIH) is one of the most important side effects of glucocorticoids. Colchicine is a medication used to manage inflammation with not yet fully understood mechanisms. This work aimed to investigate the potential protecting effect of colchicine against the development of SIH, and to spot the possible mechanisms involved in this action.

Methods: 24 adults male Wistar rats were allocated into 4 equal groups; the Control group: obtained saline, the Colchicine Group: received oral colchicine (0.5mg/kg/day) for 10 days, the SIH group: received dexamethasone (1mg/Kg/day, i.p.) for 10 days, the Colchicine-treated SIH Group: received dexamethasone for 10 days simultaneous with colchicine in the same previous doses. At the end of our experimental period, HOMA-IR, serum levels of insulin, and glucose were measured. Also, NLRP-3, ASC, gasdermin, IL-1, caspase-1, 8-OHdG, mTOR, TGF-β1, and Smad-2 were evaluated. Furthermore, histopathology of the liver and pancreas was assessed.

Results: Our study detected steroid-induced hyperglycemia with inflammation, oxidative stress, and deteriorated liver and pancreas structure. Treatment with colchicine greatly suppressed the NLRP3/ASC/gasdermin/IL-1/caspase-1 pathway. Moreover, colchicine declined TGF-β1, and Smad2 gene expression with normalization of glycemic parameters and histopathological disruption.

Conclusion: according to our findings, colchicine is proposed as a potential inhibitor of SIH.

Keywords Liver; Pancreas; NLRP-3; TGF-β1; ASC

INTRODUCTION

Glucocorticoids (GCs) are well-known anti-inflammatory and immunosuppressive drugs in various sicknesses[1], and one of the most effective glucocorticoids with a prolonged duration of action is dexamethasone. Recently, it has been recommended for acute respiratory syndrome coronavirus (COVID-19)[2]. Despite the efficacy of glucocorticoids, they frequently cause metabolic adverse effects such as diabetes, osteoporosis, and hypertension[3]. The study by Aberer et al.[4] revealed that steroid-induced hyperglycemia (SIH) is among the most important side effects of glucocorticoids.

Abnormally increased blood glucose levels that occur with the administration of GCs in patients, whether they already have diabetes mellitus (DM) or not, are referred to as SIH. Furthermore, SIH may induce new-onset hyperglycemia or aggravation of hyperglycemia in patients with known DM[5].

The molecular mechanisms responsible for GCs' effect on glucose homeostasis are composite and still not fully elucidated[6]. The studies by Geer et al.[7] and Bonaventura and Montecucco[5] reported that inducing insulin resistance, raising hepatic gluconeogenesis, decreasing peripheral insulin sensitivity, and blocking pancreatic insulin

release and synthesis are all effects of glucocorticoids. Moreover, Holness et al[8]. found that dexamethasone decreases insulin secretion from pancreatic β-cells because of oxidative stress development.

Concurring with research by Houstis et al.[9] and van Raalte et al.[10] , glucocorticoids cause reactive oxygen species (ROS) to be produced, which lowers glucose uptake at the level of adipose and muscular tissue. Moreover, Martínez et al. [11] reported that animals treated experimentally with glucocorticoid demonstrated hyperglycemia, hypoinsulinism, and reduced peripheral insulin sensitivity.

It was reported that hyperglycemia upsurges inflammatory markers and enhances oxidative stress[12,13]. The established oxidative stress and inflammation cause insulin resistance, which leads to the progression of diabetes.[14,15]

According to research by Perez et al. [3] and Suh and Park **[6]**, patients with glucocorticoid-induced hyperglycemia do not currently have access to established hypoglycemic medications or treatment plans that are efficient in establishing appropriate glycemic control and lowering the possibility of problems. Furthermore, it was said that there is insufficient data to set specific treatment objectives for SIH patients[5,16].

Colchicine (COL) is an extract from the *Colchicum autumnale* plant that appears in maize, seeds, and flowers. There is ample evidence supporting its use as a medicinal herb to relieve joint strain[17]. Moreover, it is considered a versatile, inexpensive, anti-inflammatory medication that treats and prevents gout attacks, post-pericardiotomy syndrome, familial Mediterranean fever (FMF), and pericarditis[18].

Colchicine has glucose lowering effects and may reduce the threat of type 2 DM[19,20]. It was reported that it downgrades the inflammatory reaction and improves the antioxidant capability in high-fat diet-fed rats[21]. Furthermore, it significantly improved obesity-associated inflammation and normalized fasting glucose, insulin, and insulin resistance[22].

Herein, in this study, we aimed to assess the protective consequence of colchicine against the development of SIH based on the former studies which corroborated its anti-inflammatory, anti-oxidative stress, and hypoglycemic effect. Also, we intended to spot the possible mechanism of protection.

METHODS

1.1. Drugs and rationale of dose selection

Colchicine was bought as a powder from Sigma-Aldrich, USA, and prepared in normal saline for use, while dexamethasone was obtained as ampoules containing (8 mg/2 ml) from Amriya for Pharmaceutical Industries.

Established on previous research indicating that colchicine alleviated diet-induced hyperlipidemia with normalization of inflammatory markers, oxidative stress state, and lipid profile, the dosage of (0.5mg/kg/day) of colchicine was used[23].

2.2. Experimental animals

Twenty-four adult male albino rats, 180 and 200 grams, were acquired from Faculty of Veterinary Medicine, Zagazig University in Egypt. They were sheltered in steel wire cages, six animals per cage, and kept in a hygienic environment at the animal house of Physiology Department, Faculty of Medicine, Zagazig University. The animals were accommodated at room temperature, given free access to water, fed a standard chow diet, and kept on a 12-hour light/dark cycle. Before the study started, the rats were housed in animal house for two weeks.

2.3. Ethical statement

The study followed the National Institutes of Health guidelines for the care and use of laboratory animals and was approved by Zagazig University's Institutional Animal Care and Use Committee (Zu-IACUC/2/F/36/2022).

2.4. Study design

24 rats were randomly allocated into 4 equal groups (6 rats every)

Control group [CTRL]: rats received an identical volume of normal saline intraperitoneally and by oral gavage.

Colchicine Group [CLC]: rats received colchicine (0.5mg/kg/day) by oral gavage for 10 days[24].

SIH group [SIH]: rats received dexamethasone injection (1mg/Kg/day, i.p.) for 10 days[11].

Colchicine-treated SIH Group [SIH+CLC]: rats received intraperitoneal dexamethasone injection concomitant with oral colchicine in the same previous doses and durations.

2.5. Blood and tissue Sampling

On the eleventh day of the experimentation, rats were anesthetized with thiopental (50mg/kg, i.p.), and using the method explained by Sorg and Buckner [25], blood samples were taken from each rat's retro-orbital venous plexus, collected in sterile plastic centrifuge tubes, and left to clot. The serum was then separated using a 15-minute, 3000 rpm blood centrifugation. Using fine-tipped automated pipettes, the supernatant serum was pipetted off and reserved at -20° C until it was tested for biochemical parameters.

All rats were decapitated immediately after blood sampling. The liver and pancreas were then extracted as quickly as possible and divided into 2

parts: one part of each organ was frozen in liquid nitrogen and stored at -80° C to be used for biochemical and gene expression studies, whereas the other parts were used for histopathological and immunohistochemical studies after fixation with formalin.

2.6. Biochemical study

2.6.1 Assay of glycemic indices

Serum glucose was measured using a competitive ELISA kit (MyBioSource, USA) and insulin was measured in the serum using insulin sandwich ELISA Kits (MyBioSource, USA) following instructions of the manufacturers. Estimation of Homeostatic model assessment for insulin resistance (HOMA-IR) was done using the equation: [HOMA-IR = serum insulin (µU/mL) x serum glucose (mg/dl) /405] conferring to Sun et al.[26] altered on Matthews et al.[27].

2.6.2. Determination of lipid profile

Plasma triglyceride, cholesterol, and high-density lipoprotein (HDL) were measured in serum by quantitative colorimetric method using an assay kit (Spinreact, Spain) according to the manufacturers' guidelines.

2.6.3. Assay of inflammatory mediators

Serum interlukin-1 (IL-1) was measured using an enzyme-linked Immunosorbent assay Kit (Cloud-Clone Corp, USA). Pancreatic NLR Family Pyrin Domain Containing Protein 3 (NLRP-3) assay was done using a competitive ELISA kit (MyBioSource, USA). Furthermore, serum Gasdermin was measured using an Enzyme-linked Immunosorbent Assay Kit (MyBioSource, USA). Also, serum caspase-1 was measured using an Enzyme-linked Immunosorbent Assay Kit (Cloud-Clone Corp, USA). All procedures were done following the manufacturers' guidelines.

2.6.4. Apoptotic and oxidative stress markers assay

Caspase-3 was measured in the pancreatic tissue after the preparation of homogenates using an ELISA kit (MyBioSource, Egypt) and 8-hydroxy-2-deoxyguanosine (8-OHdG) was measured in the pancreatic homogenate using an ELISA Kit (MyBioSource, Egypt) following instructions of the manufacturers.

2.6.5. Drosophila protein, mothers against decapentaplegic homolog 2 (Smad2) and transforming growth factor (TGF- β1) evaluation

Quantitative real-time PCR was used to quantify total RNA extracted from the liver tissue using the Qiagen tissue extraction kit (Qiagen, USA) agreeing with the manufacturer's instructions. TGF-β1 and Smad-2 have different primer sequences: [Forward primer: 5'-CCCAGCATCTGCAAAGCTC-3'; Reverse primer: 5'-GTCAATGTACAGCTGCCGCA-3'] and [Forward primer: 5'-CCTGCACAGCTCCAGGCACC-3'; Reverse primer: 5'-TGTCCATTGGGCTTGCG -3'], respectively.

2.6.6. Apoptosis-associated speck-like protein with a caspase recruitment domain (ASC), and mammalian target of rapamycin (mTOR)

Following the extraction of protein solutions from the pancreatic tissue, a Bio-Rad Mini-Protein II system was used to separate similar amounts of protein (20–30 µg) by sodium dodecyl sulfate–polyacrylamide gel electrophoresis (SDS-PAGE) (10% acrylamide gel). The protein was transferred using a Bio-Rad Trans-Blot technique on polyvinylidene difluoride membranes (Pierce). After that, membranes were cleaned in PBS and blocked with 5% (w/v) skim milk powder in PBS for one hour. For primary antibody responses, we adhered to the manufacturer's directions. Following blocking, the blots were produced using ASC, mTOR, and β-actin antibodies (diluted 1:1000) from Santa Cruz Biotechnology, Inc., USA. They were then rinsed and treated for one hour at 37°C with secondary antibodies labeled with peroxidase. Using ChemiDocTM imaging equipment and Image LabTM software version 5.1 (Bio-Rad Laboratories Inc.), band intensity was measured. The outcomes are normalized to the expression of the β-actin protein and then reported in arbitrary units.

2.7. Histopathological analysis of pancreatic and hepatic tissues

After being fixed in 10% neutral buffered formalin, pancreatic and hepatic tissues were embedded in paraffin. Then, sections with a thickness of 5 µm were obtained, and were mounted on glass slides, deparaffinized with xylene, and were ready for staining.

2.7.1. Hematoxylin-eosin staining (H&E) and Sirius red staining

According to **Layton and Bancroft (2018)**[28], sections were stained with hematoxylin and eosin (H&E stain) to notice the pancreatic and hepatic integrity and architecture. While slices were treated with Sirius red stain to identify collagen fibers in the liver tissues[29].

The Pathological Committee of the NASH Clinical Research Network nominated the NAFLD Activity Score (NAS), which was used to evaluate the histological grading of non-alcoholic fatty liver disease (NAFLD) after the H&E sections had been prepared and examined[30]. The following scores added up to the total: lobular inflammation (0=no foci, 1=2 foci per 200 field, 2=2-4 foci per 200 field, 3=>4 foci per 200 field), ballooning (0=none,

1=rare or few, 2=many or conspicuous), and steatosis (0=5 %, 1=5-33 %, 2=34-66 %, 3=>66 %). NASH was classified as a NAS score of ≥5, borderline NASH as a NAS score of 2–5, and simple steatosis as a NAS score of ≤2.

Furthermore, fibrosis scoring was carried out by **Kleiner et al. (2005)**[30] after the sections had been prepared and examined using Sirius red stain. Stage 1 comprises zone 3 perivenular and perisinusoidal fibrosis, which is further divided into 1a and 1b based on the amount of the deposit. Stage 1c is isolated periportal fibrosis. Stage 2 comprises portal and central fibrosis without bridging fibrosis. Stage 3 is bridging fibrosis, and stage 4 is cirrhosis. This staging strategy is widely approved due to its suitability for NAFLD-associated fibrosis[31].

2.7.2. Immunohistochemical staining

Caspase-1 and nuclear factor erythroid 2–related factor 2 (Nrf2) in the pancreatic and hepatic tissues were identified immunohistochemically using the avidin-biotin-peroxidase technique application according to the method of Kiernan [25]. In addition, pancreatic insulin and hepatic insulin receptor-1 were identified using the same technique.

Pancreatic and hepatic slices of a thickness of five µm were dewaxed, rehydrated, and cleaned using phosphate -buffered saline (PBS). Subsequently, 0.3% hydrogen peroxide was applied for 10 minutes. Following a PBS rinse, non-specific binding was inhibited by incubating in 5% normal goat serum at room temperature for one hour. The primary antibodies, anti-Caspase-1 (Catalogue No. MA5-32137, rabbit monoclonal antibody, Invitrogen, diluted at 1:200) and anti-Nrf2 (Catalogue No. A0674, rabbit polyclonal antibody, Abclonal, diluted at 1:100), were then applied to the pancreatic and hepatic sections and left overnight in a humid chamber.

The primary antibodies for insulin (Catalogue No. ab282459, rabbit polyclonal antibody, Abcam, at a dilution of 1: 10000; heat-mediated antigen retrieval with citrate buffer pH 6 was performed before starting the IHC staining protocol) and anti-insulin receptor (Catalogue No. ab137747, rabbit polyclonal antibody, Abcam, at a dilution of 1: 500) were then incubated with other pancreatic and hepatic sections during this time.

The slices were soaked in PBS three times before being incubated for an hour at room temperature with the matching biotinylated secondary antibody. Next, Streptavidin horseradish peroxidase was added and let to sit for an additional sixty minutes. Following three further PBS washes, 3,3-diaminobenzoic acid (DAB)-hydrogen peroxide was used as a chromogen to visualize immunoreactivity. Finally, slides were coated, dehydrated, and counterstained with Mayer's hematoxylin. Anti-caspase-1 has a cytoplasmic, nuclear, and cytoplasmic positive brown staining pattern; anti-Nrf2 has a cytoplasmic and nuclear pattern; and anti-insulin, cytoplasmic, and membranous.

The Leica DM500 and Leica ICC50 W Camera Modules were used for the light microscopy examination of the hematoxylin and eosin, Sirius red, and immunohistochemically stained slides at the Image Analysis Unit of the Anatomy and Embryology Department, Faculty of Medicine, Zagazig University.

2.7.3. Morphometrical analysis

The data was quantified with the public domain image-processing software "Image J" (Version 1.50, 23 April 2019). Quantification of the positive insulin-stained islet area, number of β-cell per islet (distinct nuclei surrounded by insulin-positive stained areas), and the size of β-cells per islet (insulin-stained area distributed by the number of β-cells) were measured at ×400 magnification. The quantification of the positively labeled areas of caspase-1 and Nrf2 (areas stained with brown color) in addition to the optical density of cytoplasmic Nrf2 and membranous insulin-receptor-1 were all measured at ×400 magnification. The Nrf2-positive nuclei were also calculated at ×400 magnification as well. However, the quantification of the positively labeled area of Sirius red staining (areas stained with red color) was measured at ×100 magnification.

The image analyzer was first automatically calibrated to convert the measurement units (pixels) produced by the program into actual micrometer units. Five non-overlapping, randomly chosen fields from each specimen's slide in the various groups were evaluated. The information was logged, displayed as mean ± SD, and prepared for statistical examination.

2.8. Data analysis

The SPSS software (Version 22.0) was used to verify, enter, and analyze the data. The studied groups were statistically paralleled using one-way analysis of variances. Post hoc tests were used when the ANOVA test revealed a significant difference. For multiple comparisons between groups, the Tukey's honestly significant difference (Tukey HSD) test was utilized when the data was homogeneous; in the absence of homogeneity, the Games Howell test was employed. When the p-value was less than 0.05, differences were deemed statistically significant. For non-parametric data, Kruskal Wallis test, followed by Dunn’s post hoc test was used. The results were given as mean

standard deviation (SD). Furthermore, the colchicine preventative index was computed as follows: SIH-(SIH+CLC)/SIH %.

RESULTS

The current work paraded no significant difference between the colchicine, and the control groups confirming its safety. Furthermore, throughout the experiment, there were no case fatalities reported in any of the study groups.

3.1. Biochemical results

3.1.1. Effect of colchicine on dexamethasone-induced disturbance of serum glycemic indices

Dexamethasone administration exhibited a significant ($p<0.05$) rise of serum glucose, and serum insulin besides recorded insulin resistance with HOMA-IR, compared to the control rats. colchicine administration with dexamethasone revealed a significant ($p< 0.05$) diminish in serum glucose by 43%, serum insulin by 58%, and insulin resistance by 67% as shown in **Table 1.**

3.1.2. Effect of colchicine on dexamethasone-induced disturbance of lipid profile in the serum

Dexamethasone administration exhibited a significant ($p<0.05$) rise in serum cholesterol, and serum triglycerides with a significant ($p<0.05$) decline of HDL related to the control rats. colchicine administration with dexamethasone revealed a significant ($p<0.05$) diminish in serum cholesterol by 25%, and serum triglycerides by 48% with a significant ($p<0.05$) elevation of serum HDL by 47% as shown in **Table 2.**

3.1.3. Effect of colchicine on dexamethasone-induced elevation of inflammatory markers

Dexamethasone administration indicated a significant ($p<0.05$) elevation of serum IL-1, caspase-1, and gasdermin and pancreatic NLRP-3, compared to the control rats. On the contrary, colchicine administration with dexamethasone revealed a significant ($p<0.05$) diminish in IL-1 by 56%, NLRP-3 by 63%, caspase-1 by as 25%, and gasdermin by 73% as shown in **Table 3.**

3.1.4. Effect of colchicine on dexamethasone-induced elevation of pancreatic oxidative stress and apoptotic markers

Dexamethasone administration exhibited a significant ($p<0.05$) elevation in pancreatic 8-OHdG, and caspase-3 compared to the control rats. Nevertheless, colchicine administration with dexamethasone revealed a significant ($p<0.05$) diminish in 8-OHdG by 68%, and caspase-3 by 48% as shown in **Table 4.**

3.1.5. Effect of colchicine on dexamethasone-induced elevation of pancreatic TGF-β1, and Smad2 gene expression

Dexamethasone administration exhibited significant ($p<0.05$) elevation in pancreatic TGF-β1, and Smad2 gene expression paralleled with the control rats. However, colchicine administration with dexamethasone exhibited a significant ($p<0.05$) diminish in TGF-β1, and Smad2 gene expression by 72% and 54% respectively as displayed in **Table 5.**

3.1.6. Effect of colchicine administration on dexamethasone-induced elevation of hepatic ASC, and mTOR protein expression

Dexamethasone administration exhibited a significant ($p<0.05$) rise in hepatic ASC, and mTOR protein expression compared to the control rats. However, colchicine administration with dexamethasone displayed a significant ($p<0.05$) diminish in ASC, and m-TOR protein expression by 60% and 43% respectively as displayed in **Table 6 and Fig.1.**

3.2. Histopathological results and analysis

3.2.1. Effect of colchicine on dexamethasone-induced hypertrophy and hyperplasia of insulin-secreting β-cells and the altered structure of pancreatic islets

The pancreatic section of the control and colchicine groups showed preserved lobular architecture with lightly stained islets of Langerhans surrounded by the pancreatic acini. Each pancreatic islet was formed of cell cords separated by a network of blood capillaries. The pancreatic acini showed basal basophilia and apical acidophilia. **On the contrary,** cells of the islet of Langerhans within the **SIH group** showed vacuolated cytoplasm and some with shrunken, darkly stained nuclei in addition to dilated, congested blood capillaries. Concomitant treatment with colchicine resulted in marked enhancement in the structure of the pancreatic islets with few vacuolated cells in addition to other normal polygonal cells with few dilated congested blood capillaries (**Fig. 2**).

Strong cytoplasmic immunoreactivity for insulin was seen in the most of the pancreatic islet cells in insulin-immunostained pancreatic slices from the control group, primarily in the central region. The **SIH** group showed increased insulin immunoreactivity within the pancreatic islets that were decreased in the **colchicine-treated SIH** group (**Fig. 3**).

Statistical analysis of the morphometrical results of the Insulin-immunostained pancreatic sections revealed that the insulin-positive area increased by

2.2-fold within the dexamethasone-treated rats. Meanwhile, the number and size of β-cells increased by 1.95 and 1.15 folds simultaneously with those of the control group. Coadministration of colchicine caused a significant ($p<0.05$) diminution in the size of the insulin-positive area by 36.37 %, the number of β-cells by 32.4% in relation to the **SIH** group with a non-significant diminish in the size of β-cells.

3.2.2. Effect of colchicine on dexamethasone-induced steatohepatitis and liver fibrosis using hematoxylin and eosin and Sirius-Red staining:

The hepatic sections of the control and colchicine groups showed tightly packed cords of hepatocytes with narrow blood sinusoids in between radiating from the central vein. Hepatocytes exhibited rounded vesicular nuclei and acidophilic cytoplasm with numerous binucleated hepatocytes. The-portal area contained portal vein, hepatic artery, and bile duct (Fig. 4 a-b`). Dexamethasone administration induced non-alcoholic steatohepatitis with marked micro and macro steatosis in hepatocytes represented as swollen hepatocytes with variable cytoplasmic vacuolations, either multiple defined small vacuoles, or large coalesced vacuoles (Fig. 4 c-e) with ballooning degeneration. The portal area showed dilated congested portal vein and bile duct proliferation (Fig. 4c). Mononuclear cellular infiltrations were present within the portal area (Fig. 4c), around the central vein (Fig. 4d), and within the hepatic lobules (NAS score from 5-6). Hemorrhage was present within some hepatic sections as well (not shown). Colchicine coadministration resulted in a significant ($p<0.05$) reduction of the hepatic lesions (NAS score from 2-3) and a noticeable reduction in the size of swollen hepatocytes but still with vacuolated cytoplasm. Meanwhile, some hepatocytes appeared normal. In addition, the portal area exhibited mild cellular infiltrations (Fig. 4f-f`& g).

In the control and colchicine groups, Sirius red-stained hepatic sections displayed no fibrosis (score 0) except for small amounts of collagen fiber deposition lining sinusoids, around the central vein and in the portal area. Within the **SIH** group, collagen fibers were densely deposited within the portal tract spreading to few lobular septa and around the central vein (score 2-3). On the other hand, the colchicine-treated SIH group exhibited a moderate amount of collagen fibers deposition around the central vein and within portal areas (score 1c-2) (Fig. 5).

The SIH group's area % of Sirius red positive stained area showed a statistically significant ($p<0.05$) rise when compared to the control groups. Nonetheless, there was a notable 52.8% reduction in the area of collagen fibers in colchicine treated SIH group compared to the SIH group.

3.2.3. Effect of colchicine on dexamethasone-induced hepatic insulin insensitivity using anti-insulin receptor:

Hepatic sections of the control and colchicine groups revealed strong positive anti-insulin receptor immuno-reaction on the cell membrane of hepatocytes (Fig. 6). The SIH group displayed a statistically significant ($p<0.05$) reduction in the insulin receptor immunoreactivity and reduction by 30.61% when rivaled to the control group. Instead, **colchicine-treated SIH** rats showed a statistically significant ($p<0.05$) elevation of the insulin receptor immunoreactivity concerning the **SIH** group with elevation by 20.79%.

3.2.4. Immunohistochemical analysis of caspase-1 in the hepatic and pancreatic sections and their morphometrical analysis:

Examination of caspase-1 immunostained pancreatic sections of the control and colchicine groups revealed minimal to negative immune reactions for caspase-1. Dexamethasone administration resulted in strong cytoplasmic caspase-1 immuno-reaction within the pancreatic cells; on the other hand, colchicine coadministration resulted in mild caspase-1 immunoreactivity within the pancreatic cells (Fig. 7).

Meanwhile, caspase-1 immunostained hepatic sections showed mild cytoplasmic caspase-1 immuno-reactions within the control and colchicine groups. However, within the SIH group, strong caspase-1 immunoreaction was mainly localized to non-parenchymal sinusoidal cells, and a lesser extent to hepatocytes. The colchicine-treated SIH group showed moderate caspase-1 immunoreactivity within both sinusoidal cells and hepatocytes (Fig. 7).

The statistical analysis of the area percentage of caspase-1 immunoreactivity within the pancreatic and hepatic sections of the SIH group disclosed a statistically significant ($p<0.05$) elevation compared to the control group. In addition, the colchicine-treated SIH group rats showed a statistically significant ($p<0.05$) decrease compared to the SIH group. The pancreatic and hepatic sections of the colchicine-treated SIH group revealed a reduction of 47.72%, and 63.41% respectively concerning the SIH group.

3.2.5. Immunohistochemical analysis of Nrf2 in the hepatic and pancreatic sections and their morphometrical analysis:

The nuclear related factor (Nrf2) immunostained pancreatic sections of the control, and colchicine groups revealed a brown-immunostained

cytoplasm and non-stained nuclei within almost all the pancreatic islets cells. However, the rats of the SIH group showed a marked decrease in the cytoplasmic Nrf2 with increased brown stained nuclei. The SIH group rats treated with colchicine showed a moderate cytoplasmic Nrf2 immunoreactivity with increased, brown-stained nuclei as well (Fig. 8).

Examination of the hepatic Nrf2 immunostained sections of both the control and colchicine groups revealed hepatocytes with dense brown immunostained cytoplasm and non-stained nuclei as well as other cells with dense cytoplasmic Nrf2 and brown-stained nuclei. The rats of the SIH group showed a marked decrease in the cytoplasmic Nrf2 with increased, brown-stained nuclei. Meanwhile, the rats of the colchicine-treated SIH group rats showed a moderate cytoplasmic Nrf2 immunoreactivity with increased brown stained nuclei (Fig. 8).

The statistical analysis of the morphometrical results of the SIH's Nrf2-immunostained pancreatic and hepatic sections revealed a significant ($p<0.05$) rise in the number of Nrf2-positive nuclei within the hepatocytes and pancreatic islets accompanied by decreased cytoplasmic Nrf2 immunoreactivity represented by either decreased optical density within the pancreatic islets or area percentage of Nrf2 hepatic immunoreactivity when competed to the control group. However, pancreatic, and hepatic sections of the colchicine-treated SIH group displayed a significant ($p<0.05$) difference concerning the SIH group. The number of pancreatic Nrf2-positive nuclei showed a decline of 32.4% and the optical density of cytoplasmic Nrf2 revealed elevation of 11.29% in relation to the SIH group. Meanwhile, the number of Nrf2 positive hepatic nuclei of the colchicine-treated SIH group sections revealed reduction of 37.85% and the area percentage of hepatic Nrf2 showed elevation of 70.38% in relation to the SIH group.

Table 1: Effect of colchicine administration on dexamethasone-induced disturbance of serum glycemic indices.

Groups	Control Group [CTRL]	Colchicine Group [CLC]	SIH Group [SIH]	Colchicine-treated SIH Group [SIH+CLC]
Serum glucose (mg /dl)	83.75±5.37 **a**	84.68±0.61 **a**	231.1±1.12 **b**	130.28±0.38 **b, c**
Serum insulin (µIU/ml)	6.03±1.21 **a**	6.54±0.89 **a**	18.76±0.95 **b**	7.72±0.55 **c**
HOMA-IR	1.24±0.27 **a**	1.35±0.22 **a**	10.69±0.57 **b**	2.48±0.21 **b, c**

Results expressed as mean ± SD (N=6). Data was analyzed by ANOVA followed by the Games-Howell post hoc test.

a control and colchicine groups, **b** significant ($P<0.05$) versus control and colchicine groups, **c** significant ($p<0.05$) versus SIH group

HOMA-IR: Homeostatic model assessment for insulin resistance

Table 2: Effect of colchicine administration on dexamethasone-induced disturbance of lipid profile in the serum

Groups	Control Group [CTRL]	Colchicine Group [CLC]	SIH Group [SIH]	Colchicine-treated SIH Group [SIH+CLC]
Cholesterol (mg/dl)	148.22±0.34 **a**	147.84±0.11 **a**	220.03±0.17 **b**	163.15±0.09 **b, c**
Triglycerides (mg/dl)	54.88±0.33 **a**	53.21±0.12 **a**	122.03±0.42 **b**	63.34±0.01 **b, c**
HDL (mg/dl)	56.34±0.22 **a**	54.87±0.04 **a**	22.01±0.43 **b**	42.26±0.03 **b, c**

Results expressed as mean ± SD (N=6). Data was analyzed by ANOVA followed by the Games-Howell post hoc test.

a control and colchicine groups, **b** significant ($p<0.05$) versus control and colchicine groups, **c** significant ($p<0.05$) versus SIH group
HDL**:** High density lipoprotein

Table 3: Effect of colchicine administration on dexamethasone-induced elevation of inflammatory markers

Groups	Control Group [CTRL]	Colchicine Group [CLC]	SIH Group [SIH]	Colchicine-treated SIH Group [SIH+CLC]
Serum IL-1 (pg/mg protein)	22.68±1.12 **a**	21.09±1.40 **a**	176.0±1.09 **b**	76.20±1.11 **b, c**
Pancreatic NLRP3 (ng/mg protein)	1.597±0.12 **a**	1.62±0.14 **a**	8.759±0.69 **b**	3.208±0.41 **b, c**
Serum Caspase-1 (pg/ml)	41.18±0.04 **a**	39.34±0.55 **a**	84.22±1.30 **b**	63.13±0.92 **b, c**
Serum Gasdermin (ng/ml)	0.84±0.03 **a**	0.82±0.91 **a**	5.67±0.32 **b**	1.49±0.54 **b, c**

Results expressed as mean ± SD (N=6). Data was analyzed by ANOVA followed by the Games-Howell post hoc test.
a control and colchicine groups, **b** significant ($p<0.05$) versus control and colchicine groups, **c** significant ($p< 0.05$) versus SIH group
IL-1: interleukin 1, NLRP3: NLR Family Pyrin Domain Containing Protein 3

Table 4: Effect of colchicine administration on dexamethasone-induced elevation of pancreatic oxidative stress and apoptotic markers

Groups	Control Group [CTRL]	Colchicine Group [CLC]	SIH Group [SIH]	Colchicine-treated SIH Group [SIH+CLC]
8-OHdG (ng/mg protein)	0.534±0.063 **a**	0.414±0.058 **a**	4.366±0.33 **b**	1.362 ±0.069 **b, c**
Caspase-3 (ng/mg protein)	0.746±0.071 **a**	0.706±0.082 **a**	5.277±0.352 **b**	2.725±0.343 **b, c**

Results expressed as mean ± SD (N=6). Data was analyzed by ANOVA followed by the Games-Howell post hoc test.
a control and colchicine groups, **b** significant ($p<0.05$) versus control and colchicine groups, **c** significant ($p<0.05$) versus SIH group 8-OHdG: 8-hydroxy 2-deoxyguanosine

Table 5: Effect of colchicine administration on dexamethasone-induced elevation of hepatic Smad2, and TGF- β1 gene expression

Groups	Control Group [CTRL]	Colchicine Group [CLC]	SIH Group [SIH]	Colchicine-treated SIH Group [SIH+CLC]
TGF-β1	0.974±0.0857 **A**	0.9575±0.244 **a**	7.398±1.019 **b**	2.065±0.276 **b, c**
Smad2	1.074±0.173 **A**	0.9278±0.1919 **a**	7.306±1.169 **b**	3.294±0.6321 **b, c**

Results expressed as mean ± SD (N=6). Data was analyzed by ANOVA followed by the Games-Howell post hoc test.
a control and colchicine groups, b significant ($p<0.05$) versus control and colchicine groups, c significant ($p< 0.05$) versus SIH group
TGF- β1: transforming growth factor, Smad2: Drosophila protein, mothers against decapentaplegic homolog 3

Table 6: Effect of colchicine administration on dexamethasone-induced elevation of pancreatic ASC, and mTOR protein expression

Groups	Control Group [CTRL]	Colchicine Group [CLC]	SIH Group [SIH]	Colchicine-treated SIH Group [SIH+CLC]
ASC	0.96±0.06 **A**	0.94±0.43 **a**	3.89±0.003 **b**	1.52±0.70 **b, c**
mTOR	0.80±0.43 **a**	0.81±0.006 **a**	4.11±0.29 **b**	2.33±0.01 **b, c**

Results expressed as mean ± SD (N=6). Data was analyzed by ANOVA followed by the Games-Howell post hoc test.

a control and colchicine groups, b significant ($p<0.05$) versus control and colchicine groups, c significant ($p<0.05$) versus SIH group

ASC: apoptosis associated speck-like protein with a caspase recruitment domain, mTOR: mammalian target of rapamycin

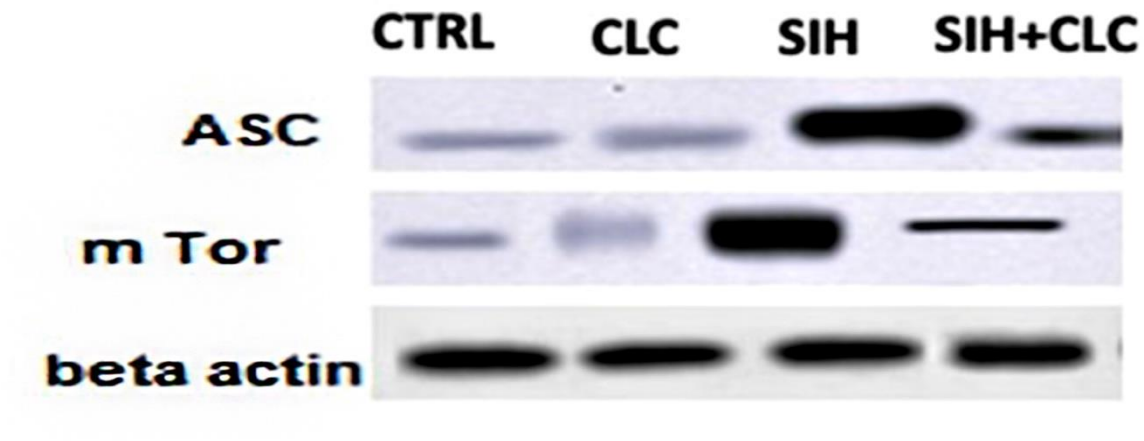

Figure 1: Effect of colchicine administration on dexamethasone-induced elevation of hepatic ASC, and mTOR protein expression

Results expressed as mean ± SD (N=6). Data was analyzed by ANOVA followed by Games-Howell post hoc test. CTRL control group, CLC colchicine group, SIH steroid induced hyperglycemia group, SIH+CLC colchicine treated SIH group ASC: apoptosis associated speck-like protein with a caspase recruitment domain, mTOR: mammalian target of rapamycin

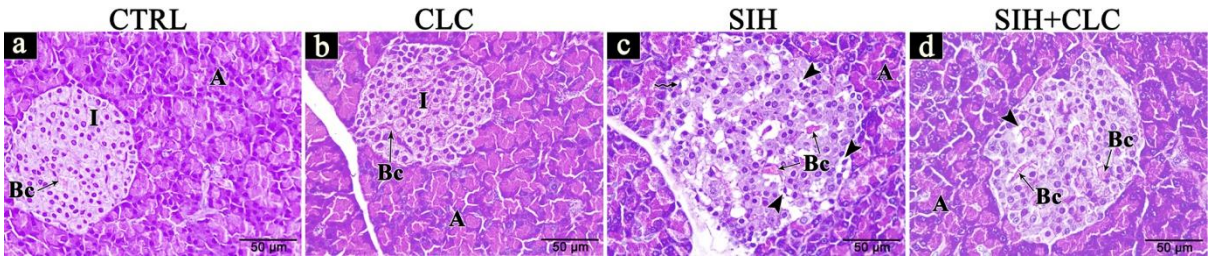

Figure 2: Illustrative images of H&E-stained pancreatic sections of different experimental groups. Pancreatic sections of the CTRL [a] and CLC [b] groups show normal lobular architecture with lightly stained islets of Langerhans (I) surrounded by the pancreatic acini (A). Cell cords forming the pancreatic islets are separated by a network of blood capillaries (BC). [c] pancreatic islets of the SIH group show cells of vacuolated cytoplasm (Arrowhead) and some with shrunken, darkly stained nuclei (Zigzag arrow). There are dilated congested blood capillaries (BC) in between cells. However, marked enhancement in the structure of the pancreatic islets of the SIH+CLC group [d] is seen with few vacuolated cells (Arrowhead) in addition to other normal polygonal cells with few dilated congested blood capillaries (BC). Notice the pancreatic acini (A)with its basal basophilia and apical acidophilia in all sections. Magnification x400 with scale bar = 50 µm

CTRL control group, CLC colchicine group, SIH steroid induced hyperglycemia group, SIH+CLC colchicine treated SIH group

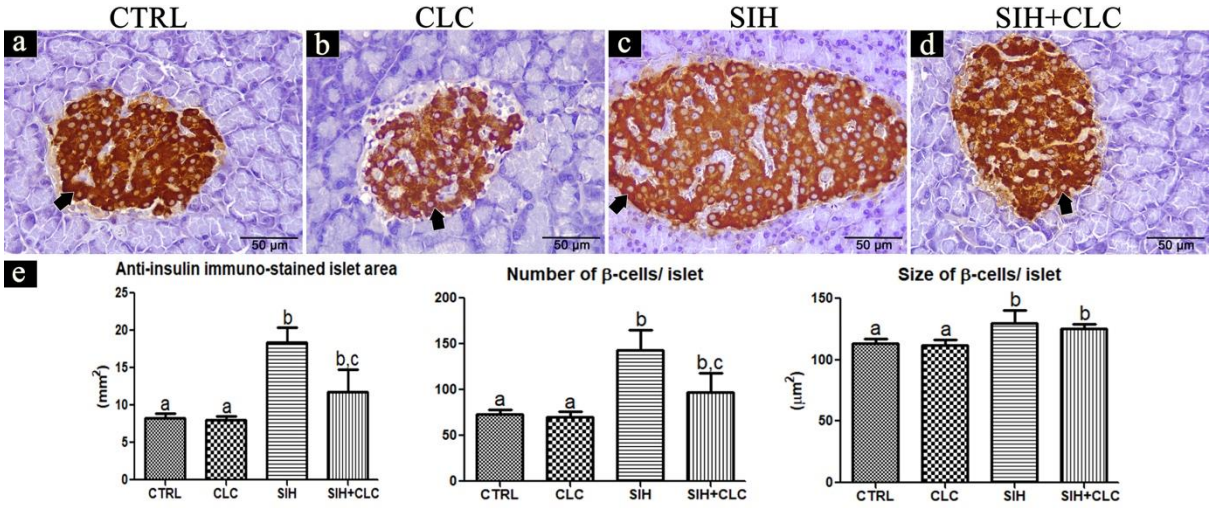

Figure 3: Illustrative images of insulin immunostained pancreatic sections of different experimental groups: [a] CTRL, [b] CLC, [c] SIH, and [d] SIH+CLC groups. The Arrow demonstrates the active insulin secreting β-cells of Langerhans Islets. Magnification x400 with scale bar = 50 µm.
[e] Bar graphs showing anti-insulin immune-stained islet area with number and size of β-cells.
Data were expressed as Mean ± SD (N=6) and analyzed by ANOVA, followed by Tukey HSD post hoc testCTRL control group, CLC colchicine group, SIH steroid induced hyperglycemia group, SIH+CLC colchicine treated SIH group ,a control and colchicine groups, b significant ($p<0.05$) versus control and colchicine groups, c significant ($p<0.05$) versus SIH group

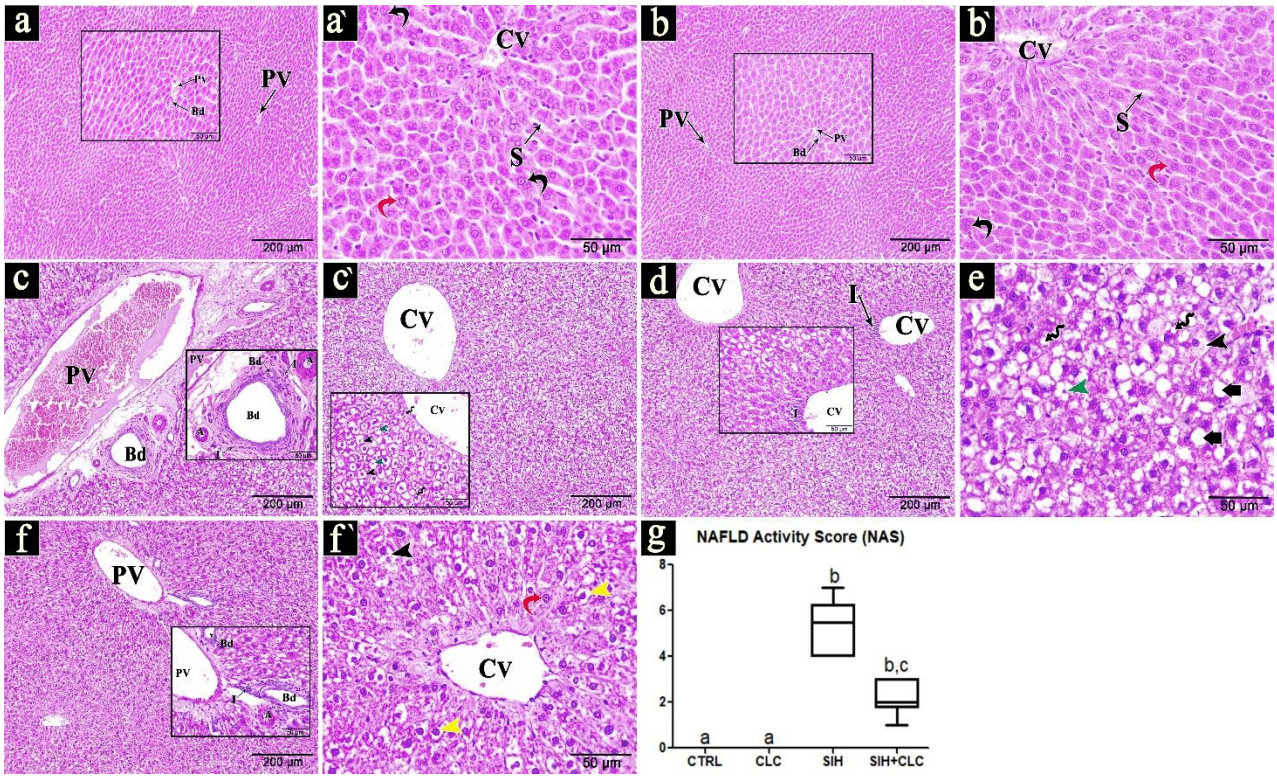

Figure 4: Representative photomicrographs of H&E-stained sections of the liver of experimental rats. Hepatic sections of both; the CTRL [a-a`] and the CLC [b-b`] groups showing part of a hepatic lobule with central vein (CV) and tightly packed cords of hepatocytes with narrow radiating blood sinusoids (S) in between. Hepatocytes exhibit rounded vesicular nuclei and acidophilic cytoplasm (Red curved arrow) with numerous binucleated hepatocytes (black curved arrow). The portal area exhibits portal vein (PV) and bile duct (Bd). SIH group [c-e] showing disturbed hepatic architecture with enlarged, rounded, swollen-appearing ballooned

hepatocytes with variable cytoplasmic vacuolations, either foamy cytoplasm (Black Arrowhead), multiple defined small vacuoles (Zigzag arrow) or large coalesced vacuoles (Short thick Arrow). Some hepatocytes have shrunken, dark-stained nuclei (Green Arrowhead). The central vein (CV) is dilated, and portal area shows hepatic artery (A), dilated, congested portal vein (PV), and bile duct proliferation (Bd). Notice the mononuclear cellular infiltration (I) within the portal area and around the central vein. The SIH+CLC [f-f `] shows marked preservation of the hepatic architecture with smaller hepatocytes having vacuolated cytoplasm (yellow Arrowhead) and other swollen hepatocytes (Black Arrowhead) surrounding slightly dilated central vein (CV) and other nearly normal hepatocytes (Red curved arrow). The portal area shows slightly dilated, congested portal vein (PV), bile ducts (Bd), hepatic artery (A), and few inflammatory cells (I). Magnification x100 and x400 with scale bars = 200 µm and 50 µm respectively.

[g] Boxplot graph shows NAFLD activity score (NAS) with data expressed as median (maximum-minimum). CTRL control group, CLC colchicine group, SIH steroid induced hyperglycemia group, SIH+CLC colchicine treated SIH group .Data was analyzed by Kruskal Wallis test, followed Dunn's post hoc test, a: Control groups; b: Significant ($p < 0.05$) versus control group and c: Significant ($p < 0.05$) versus SIH group.

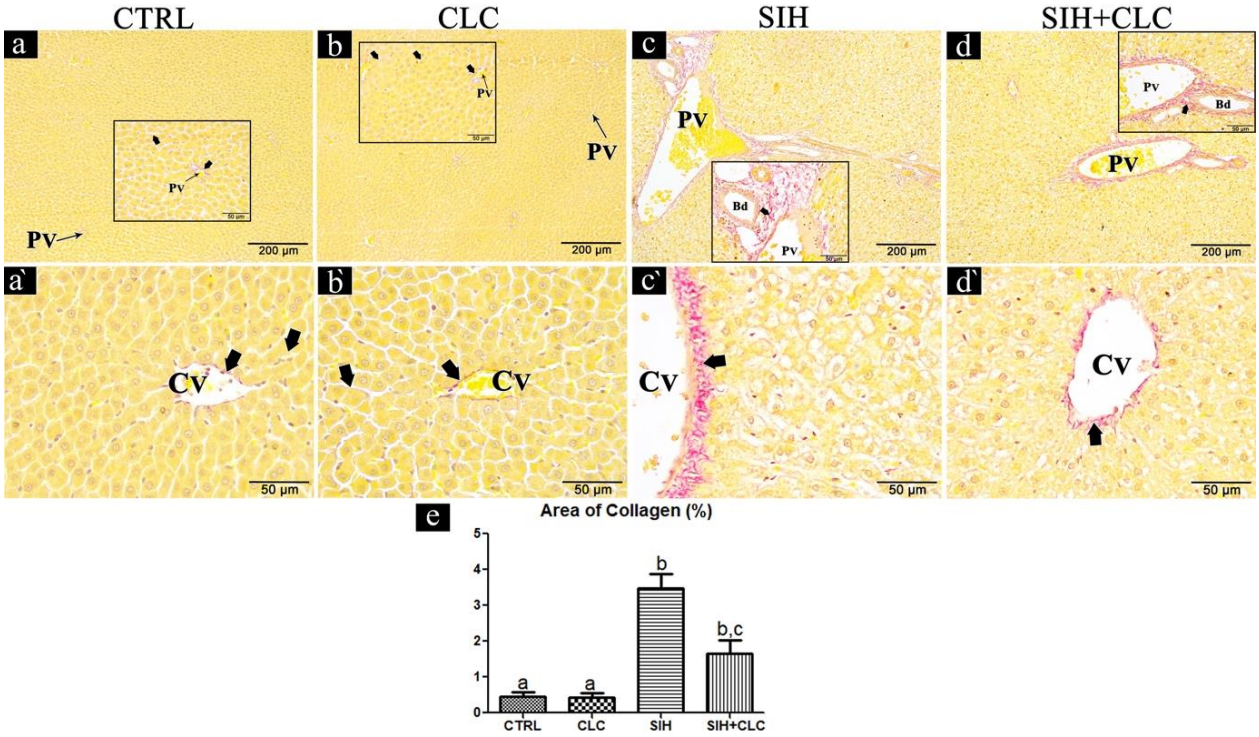

Figure 5: Illustrative images of Sirius red-stained hepatic sections showing the collagen fibers distribution in different experimental groups: [a&a`] CTRL, [b&b`] CLC, [c&c`] SIH, and [d&d`] SIH+CLC groups. The Arrow indicates red stained collagen fibers lining the sinusoids, around central vein (CV), and within the portal area around portal vein (PV) & bile ducts (Bd). Magnification x400 and x100 with scale bars = 50µm and 200µm respectively and inset magnification x400.

[e] Data was expressed as Mean ± SD (N=6) and analyzed by ANOVA, followed by Tukey HSD post hoc testCTRL control group, CLC colchicine group, SIH steroid induced hyperglycemia group, SIH+CLC colchicine treated SIH group a control and colchicine groups, b significant ($p<0.05$) versus control and colchicine groups, c significant ($p<0.05$) versus SIH group

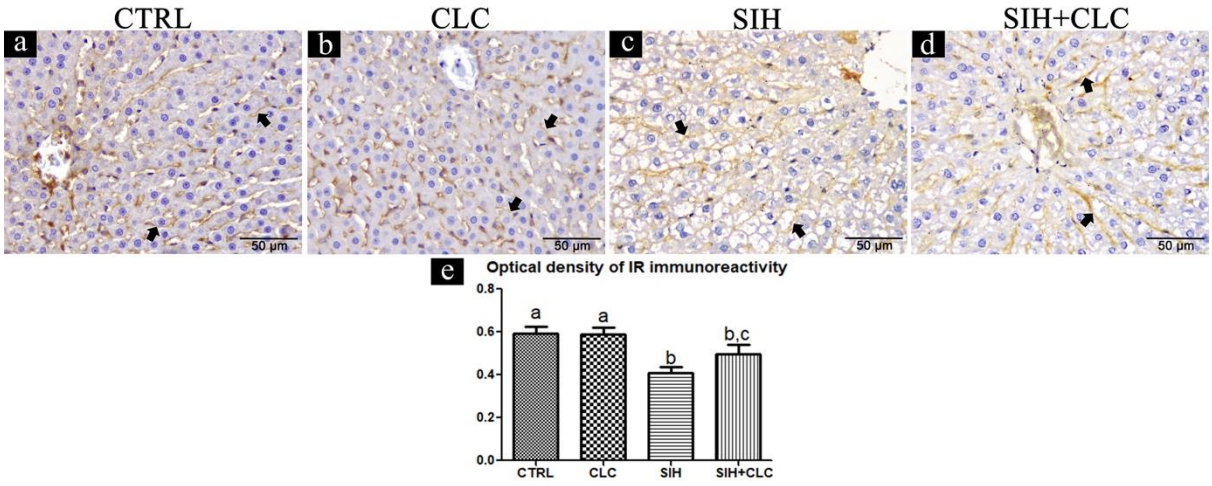

Figure 6: Illustrative images of hepatic sections showing insulin receptor immunoreactivity in different experimental groups: [a] CTRL, [b] CLC, [c] SIH, and [d] SIH+CLC groups. The Arrow signifies the positive immuno-reaction on the cell membrane of hepatocytes. Magnification x400 with scale bar = 50 µm.[e] Data was expressed as Mean ± SD (N=6) and analyzed by ANOVA, followed by Tukey HSD post hoc testCTRL control group, CLC colchicine group, SIH steroid induced hyperglycemia group, SIH+CLC colchicine treated SIH groupa control and colchicine groups, b significant ($p<0.05$) versus control and colchicine groups, c significant ($p<0.05$) versus SIH group

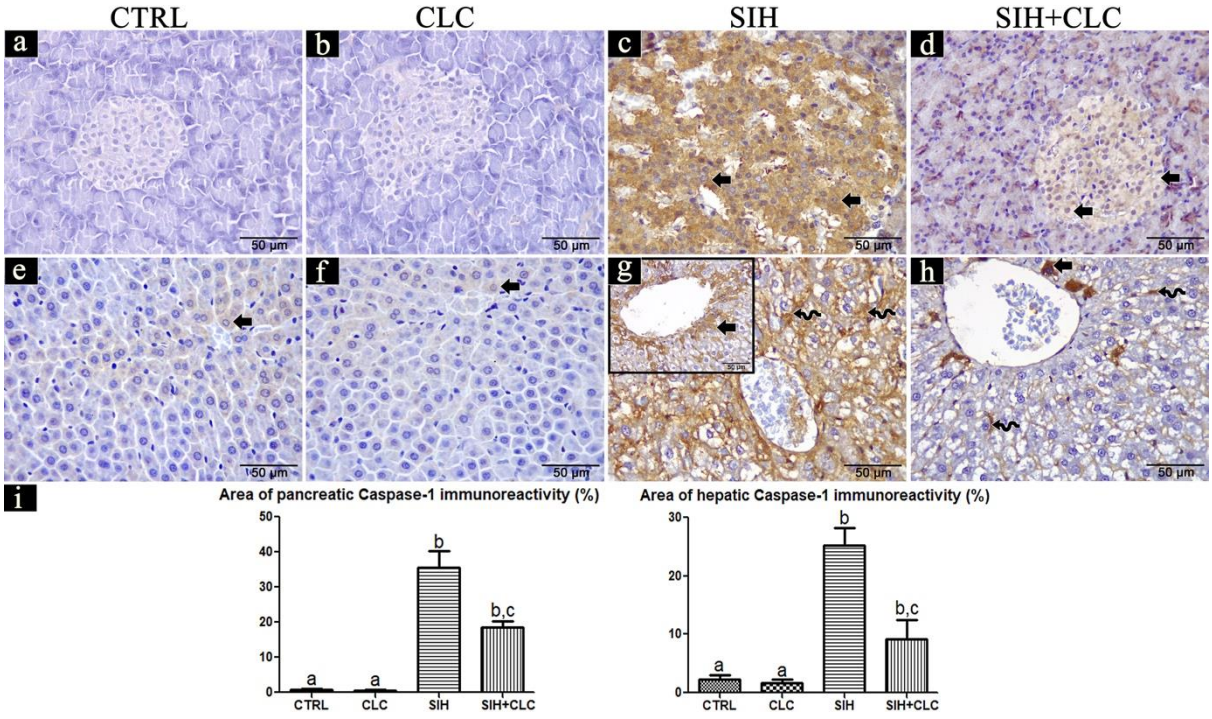

Figure 7: Illustrative images of pancreatic [a-d] and hepatic [e-h] sections showing caspase-1 immunoreactivity in different studied groups: [a,e] CTRL, [b,f] CLC, [c,g] SIH, and [d,h] SIH+CLC groups. The Arrow signifies cells with brown immunostained cytoplasm either pancreatic cells or hepatocytes, while the zigzag Arrow within hepatic sections indicates brown immunostained non-parenchymal sinusoidal cells. Magnification and inset magnification x400 with scale bar = 50 µm.
[i] Bar graphs showing area percentage of pancreatic and hepatic Caspase-1 immunoreactivity.
Data was expressed as Mean ± SD (N=6) and analyzed by ANOVA, followed by Tukey HSD post hoc test
CTRL control group, CLC colchicine group, SIH steroid induced hyperglycemia group, SIH+CLC colchicine treated SIH group

a control and colchicine groups, b significant ($p<0.05$) versus control and colchicine groups, c significant ($p<0.05$) versus SIH group

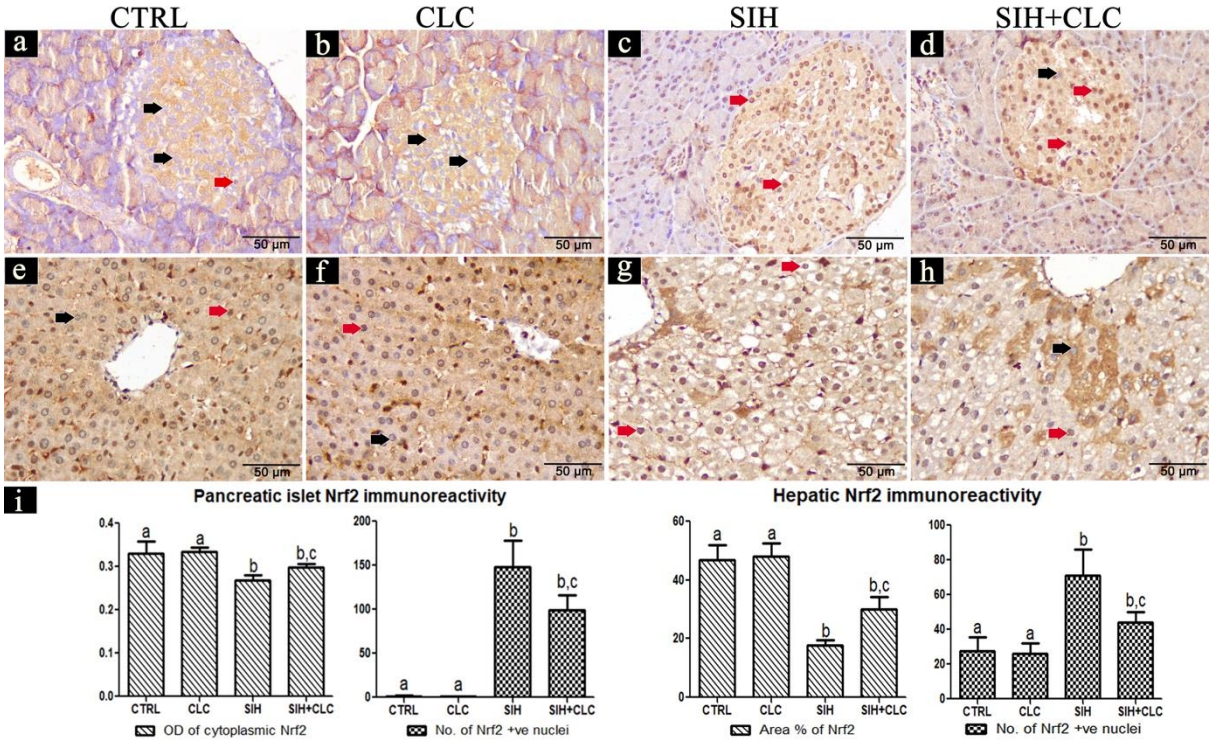

Figure 8: [a-d] Illustrative images of pancreatic [a-d] and hepatic [e-h] sections showing Nrf-2 (Nuclear factor erythroid 2–related factor 2) immunoreactivity in different studied groups: [a,e] CTRL, [b,f] CLC, [c,g] SIH, and [d,h] SIH+CLC groups. The Black Arrow signifies cell with brown immunostained cytoplasm and no staining within the nuclei, while the Red Arrow indicates cells with brown immune-stained nuclei. Magnification x400 with scale bar = 50 µm.
[i] Bar graphs showing the number of pancreatic islets' Nrf2 positive nuclei and optical density (OD) of cytoplasmic Nrf2 as well as number of Nrf2 positive nuclei and area percentage of hepatic Nrf2 immunoreactivity. Data was expressed as Mean ± SD (N=6) and analyzed by ANOVA, followed by Tukey HSD post hoc test, but Games Howell test was used for pancreatic Nrf2 positive nuclei.
CTRL control group, CLC colchicine group, SIH steroid induced hyperglycemia group, SIH+CLC colchicine treated SIH group a control and colchicine groups, b significant ($p<0.05$) versus control and colchicine groups, c significant ($p<0.05$) versus SIH group

DISCUSSION

Glucocorticoids represent repeatedly praised and habitually indispensable immunosuppressant and anti-inflammatory agents approved in innumerable medicinal situations[1,2,3], and however they have great medical efficacy**,** they persist to be abiding challenge, as they have disturbing metabolic effects as hypertension, osteoporosis, and diabetes[3]. In this context, Aberer et al**.[4]** revealed that steroid-induced hyperglycemia (SIH) is among the most important glucocorticoid side effects.

The current study is expected to research the potential protective impact of colchicine against SIH and to shed light on its possible mechanism of action.

Dexamethasone administration, 1mg/kg/day for 10 days, indicated a significant rise in serum glucose, and insulin, with increased insulin resistance accompanied with a significant disturbance of lipid profile. Inflammation was evidenced by the increase of serum caspase-1, IL-1, and gasdermin levels, pancreatic NLRP-3 level, TGF-β1, and Smad2 gene expression, and hepatic ASC, and mTOR protein expression. Furthermore, increase of pancreatic 8-OHdG and caspase-3 levels indicating oxidative stress and the resultant apoptosis. Histopathological disorientation was shown with lessened expression of cytoplasmic

Nrf2, and augmented expression of caspase-1 and anti-insulin antibodies. Colchicine administration with dexamethasone prevented all the consequential effects caused by dexamethasone, signifying its ameliorative effect.

In this current study, dexamethasone administration resulted in high serum glucose, and high insulin levels with insulin resistance indicated by elevated HOMA-IR, and based on a previous study, Barel et al.[33] revealed that rats treated with dexamethasone (1mg/kg/day, i.p.) for 10 days, expressed hyperglycemia, hyperinsulinemia with insulin resistance, and this may be because the pancreatic β-cells have augmented their function to manage the decreased insulin sensitivity caused by dexamethasone.

Additionally, van Raalte et al.[10] demonstrated that prednisolone administration induced both hyperinsulinemia and hyperglycemia leading to pancreatic beta cell failure. Moreover, the study led by Perez et al**.[3]** implied that both intravenous and oral administration of corticosteroids triggered hyperglycemia in animal models, which was explained by that steroid administration reduced glucose uptake in fatty and muscle tissue. Moreover, Shpilberg et al.[34] stated that rats which received exogenous corticosteroids together with a high fat-diet exhibited hyperglycemia with insulin resistance.

In addition, our current study showed that there was significant hyperinsulinemia, the result which is on contrary to Martinez et al.[11, who showed that dexamethasone (1mg/kg/day) caused decreased insulin levels which may be due to pancreatic beta cell destruction by the consequent oxidative stress.

Lipid profile, in our study, showed great disturbance in the form of high triglyceride, and cholesterol levels with low HDL level, and this is in line with Arab Dolatabadi et al. [35] who studied the influence of dexamethasone (0.4, 0.7, and 1 mg/ kg), given as intraperitoneal inoculation (1 ml/day) on lipid profile, and confirmed that dexamethasone increased triglyceride, cholesterol and decreased HDL levels.

In our current study, dexamethasone administration was associated with severe inflammation indicated by increased serum IL-1, gasdermin, caspase-1 levels and pancreatic NLRP-3 level. In this context, Feng et al**.[**36] conveyed that incubation of hippocampal microglia for 24 hours with dexamethasone triggered NLRP-3 activation with elevation of nuclear factor kappa B (NF-κB1), cleaved caspase-1, IL-18, and IL-1 and as well known, inflammation induce insulin resistance leading to the elaboration of [14,15]·

Additionally, Wang et al.[37]demonstrated that NLRP3/gasdermin-mediated pyroptosis was motivated with dexamethasone being used in different concentrations (0.1, 1, 10 μM) with myotubes for 24 hours. It is worth saying that ASC expression is increased as a part of inflammatory pathway triggering.

As presented in our research, dexamethasone treatment increased pancreatic 8-OHdG and caspase-3 signifying the occurrence of oxidative stress and apoptosis, and as shown in a previous research study, Zhang et al.[38]confirmed that osteoblasts incubated with dexamethasone for 24 hours showed elevated 8-OHdG, cleaved caspase-3 with decreased Nrf2 immunoexpression implying oxidative stress and apoptosis triggered by steroid treatment.

TGF-β1 endorses the emergence of inflammation and triggers fibroblast proliferation. The control of Smad proteins and their signal transduction are necessary for TGF-β1 function to be fulfilled[39]. In this context, Our research product proved that dexamethasone administration was associated with increased smad2/TGFβ-1 gene expression representing the resultant inflammation and fibrosis upon steroid injection. This result is coherent with Feng et al. [40], who showed that A549 cells, when treated with 0.1–10.0 mmol/l dexamethasone for 48 h, established an increase in TGF-β1 expression, Smad2, and caspase-3. Controversially, Shi et al.[41] stated that dexamethasone (0.45 mg/kg), can mitigate bleomycin-induced lung fibrosis in mice via attenuation of TGF-β1/Smad pathway, the effect which may be explained by the small dose used in this model compared to the dose used in ours.

The mammalian target of rapamycin (mTOR) is a serine/threonine kinase which regulates the initiation of new protein translation and subsequent translation[42]. Dexamethasone administration in our current research was accompanied by hepatic mTOR increased protein expression, the result which is in line with Alhaddad et al**.[**43**]** who showed that dexamethasone, given for 21 days, in a dose of (20mg/kg), increased mTOR protein expression inducing depression in a mice model.

Colchicine is an anti-inflammatory and antioxidant microtubule-disrupting agent[44,45]. Furthermore, it has glucose-lowering properties that may decrease the frequency of type 2 diabetes, according to a study by Nidorf et al.[20]. Colchicine was found to reduce fasting insulin resistance in obese adults, which may lower the incidence of type 2 diabetes[22,46]. These findings are consistent with the current study which confirmed that colchicine improved SIH through

normalization of glycemic indices together with the decrease of pancreatic 8-OHdG, caspase-3, serum IL-1, caspase-1, gasdermin, and pancreatic NLRP-3. Furthermore, it decreased TGF-β1, Smad2 gene expression. Also, hepatic ASC and mTOR protein expression was lessened together with the improvement of histopathological outcome.

In our current work, colchicine showed improvement of lipid profile disturbance triggered with dexamethasone, and this result was reliable with Zălar et al. [24] who studied the effect of colchicine (0.5 mg/kg) on high-fat diet-fed rats, and confirmed that it diminished TG, LDL, cholesterol levels with HDL level improvement. Also, in the same dose, it showed an anti-inflammatory effect by decreasing IL-1, tumor necrosis factor (TNF-α), and IL-6. In addition, it showed an anti-oxidative stress role as it reduced the level of malondialdehyde (MDA) with reduced glutathione (GSH) upregulation, this effect may explain the decrease of pancreatic 8-OHdG with colchicine administration in our research.

In addition, according to similar animal research, colchicine induced the antioxidant system to reduce oxidative stress in the serum and leucocytes of familial Mediterranean fever patients who were in remission [21], and this effect may also explain the cause of pancreatic 8-OHdG downregulation in our present work.

Our current research showed that colchicine suppressed the inflammatory pathway ASC/IL-1/caspase-1/gasdermin/NLRP-3, The outcome which is consistent with Robertson et al[47] who showed that colchicine, in a dose of 1mg/kg, abrogated the increase of IL-1, IL-18, NLRP-3, and caspase-1 in acute coronary syndrome patients indicating its anti-inflammatory role. Additionally, Shen et al.[48] proved that colchicine treatment (0.1 mg/kg), was associated with the downregulation of the NLRP-3 pathway in the heart failure rat model.

The NLRP-3 inflammasome is considered the crucial objective of colchicine in acute inflammation stages[44,49]as inhibiting NLRP-3 reduces IL-1, and IL-6 levels[50]. Also, the NLRP-3 inflammasome is essential to the elaboration of insulin resistance in type 2 diabetes, but its function in autoimmune type 1 diabetes is yet unknown [51,52]. Furthermore, Vandanmagsar et al. stated that NLRP-3 decrease is associated with decreased insulin resistance.

In our present study, caspase-3, an indicator of apoptosis, decreased when colchicine was administered with dexamethasone. This is consistent with Zhang et al[3] findings, which established that oral colchicine (0.5 mg/kg) significantly attenuated the expression of caspase-3 cleavage, Bax expression, heme oxygenase-1, and signal transducer and activator of transcription 3 (STAT-3).

According to our research, elevated glucose levels stimulate the transcriptional co-regulator p300, which in turn causes Smad2 acetylation to enhance TGF-β1 activity. Organ fibrosis and hypertrophy are frequently linked to the pro-sclerotic cytokine TGF-β1[54]. Furthermore, it is known that p300 acetylates Smad2 in a manner that is dependent on TGF-β1. Acetylation of Smad2 results in a conformational shift that facilitates transcription and DNA binding[55,56].

In this context, Suryono et al. [57] stated that colchicine could reduce TGF-β1, and consequently, smad2, inhibiting the cascade which regulates the deposition of fibrous tissue, and the expression of extracellular matrix protein genes in S-T elevation myocardial infarction patients, the result which confirmed that colchicine can protect against fibrosis development.

The development of cellular senescence can result from the buildup of damaged proteins and organelles brought on by the mTOR pathway's negative regulation of autophagy. Reducing ROS levels and enhancing mitochondrial function can be achieved by blocking mTOR activity[58]Colchicine administration, in our present work, caused hepatic mTOR decreased protein expression, the result which is coherent with Zhou et al. [59] who stated that colchicine prevented oxidative stress and endothelial senescence associated with depression mTOR pathway.

In our present study, SIH resulted in structural changes of the pancreatic islets cells in addition to dilation of blood capillaries. This finding is coherent with the findings of Dai et al[60]. , who established that the islet vascularization associated with insulin resistance was mediated by dilatation of preexisting arteries rather than angiogenesis. Moreover, pancreatic islets increased insulin secretion and expanded the β-cells mass in the form of β-cell hyperplasia and hypertrophy, as a complicated series of modifications to adjust to insulin resistance. This is in harmony with Rafacho et al[61]., who conveyed that hypertrophy of β-cells in dexamethasone-treated rats were linked to increased β-cell mass. These compensatory changes are crucial to ensure the appropriate circulating insulin levels that maintain blood glucose levels within normal or nearly normal physiological ranges and prevent diabetes[59]. Instead, colchicine administration to the SIH rats

resulted in enhancement of the pancreatic structure and the β-cell hyperplasia.

In the current study, dexamethasone caused central and portal fibrosis, as well as non-alcoholic steatohepatitis with pronounced hepatocyte ballooning. Ballooned hepatocytes are thought to be a diagnostic feature of NASH and have a significant effect in the pathophysiology of the disease[62,63]. They are typically first observed in zone 3, close to the central vein[64]. According to Lackner et al.**[**65] ballooned hepatocytes are supposed to be a unique type of "cell degeneration" characterized by cellular enlargement, loss of cellular polarity, a plenty of intracellular lipids, and oxidized phospholipids[65]. Several studies have examined the correlation between fibrosis stage and hepatocytic ballooning, indicating a relationship between these two histological characteristics[66]**.** Sonic hedgehog (SHH), a fibrogenic chemokine secreted by these cells, influences cell survival through an autocrine process[67] Additionally, the existence of ballooned hepatocytes may forecast the future course of liver fibrosis[68] and indicate a higher risk of disease progression[69]. However, colchicine alleviated hepatocyte ballooning, steatosis, and fibrosis caused by dexamethasone, while also impacting the NAS score. This is in line with Zălar et al**.** findings, which indicated that colchicine might reduce hepatic fat accumulation but without changing the NAS score in a high-fat diet mode[24]**.**

Within the present analysis, NASH was associated with immunohistochemically detected hepatic caspase-1 activation. This is reliable with Dixon et al[70] who reported that in their rat model of NASH and selective depletion of Kupffer cells, Kupffer cells, as one of the non-parenchymal hepatic cells, were the primary source of active caspase-1. Furthermore, caspase-1 activation in Kupffer cells led to the stimulation of proinflammatory signaling and motivation of hepatic stellate cells, which in turn caused collagen deposition and fibrosis[70].

In the undercurrent study, treatment with dexamethasone resulted in a reduction in insulin receptors. According to Abdul-Hay et al**.** [71] hyperinsulinemia causes insulin receptor down-regulation (adaptation to persistently high insulin levels), which interferes with hepatic insulin signaling and causes insulin resistance and glucose intolerance[71[. On the other hand, coadministration of colchicine with dexamethasone partially preserved the insulin receptors.

Our results suggested that SIH was tempered with colchicine by affecting the ASC/NLRP-3/caspase-1/IL-1/gasdermin pathway accompanied with downregulation of the TGF-β1/Smad2 pathway, and this is considered a logically accepted effect of the colchicine being an important anti-inflammatory agent.

CONCLUSION

Our existing work provides loads of evidence that propose that disrupting the NLRP-3/caspase-1/IL-1/gasdermin pathway with downregulation of the TGF-β1/Smad2 pathway could impair the hyperglycemic effect caused by dexamethasone administration.

Conflict of Interest: None
Financial Disclosure: None

REFERENCES

1- Cui A., Fan H., Zhang Y., Zhang Y., Niu D., Liu S., et al.: Dexamethasone-induced Krüppel-like factor 9 expression promotes hepatic gluconeogenesis and hyperglycemia. Clin. Invest 2019., **129(6):** 2266-78.

2-Wiersinga W.J., Rhodes A., Cheng A.C., Peacock S.J., and Prescott H.C. : Pathophysiology, Transmission, Diagnosis, and Treatment of Coronavirus Disease 2019 (COVID-19): A Review. JAMA 2020 , **324:** 782–93.

3-Perez A., Jansen-Chaparro S., Saigi I., Bernal-Lopez M.R., Minambres I., and Gomez-Huelgas R. : Glucocorticoid-induced hyperglycemia. J. Diabetes 2014 , **6:** 9-20.

4- Aberer F., Hochfellner D. A., Sourij H., and Mader J.K.: A Practical Guide for the Management of Steroid Induced Hyperglycaemia in the Hospital. J. Clin. Med. 2021, **10(10):** p2154

5-Bonaventura A., and Montecucco F. : Steroid-induced hyperglycemia: An underdiagnosed problem or clinical inertia? A narrative review. Diabetes Res. Clin. Pract. 2018, **139:** 203–20.

6- Suh S., and Park M.K.: Glucocorticoid-Induced Diabetes Mellitus: An Important but Overlooked Problem. Endocrinol Metab (Seoul) 2017 , **32(2):**180-9.

7- Geer E.B., Islam J., and Buettner C. : Mechanisms of glucocorticoid-induced insulin resistance: Focus on adipose tissue function and lipid metabolism. Endocrinol. Metab. Clin. N. Am. 2014, **43:** 75–102.

8- Holness M.J., Smith N.D., Greenwood G.K., and Sugden M.C. : Interactive influences of peroxisome proliferator-activated receptor alpha activation and glucocorticoids on pancreatic beta cell compensation in insulin resistance induced by

dietary saturated fat in the rat. *Diabetologi 2005a* ,**48(10):** 2062–68.

9- Houstis N., Rosen E.D., and Lander E.S. (2006): Reactive oxygen species have a causal role in multiple forms of insulin resistance. Nature, **440(7086):** 944-52.

10- van Raalte D.H., Ouwens D.M., and Diamant M. : Novel insights into glucocorticoid-mediated diabetogenic effects: towards expansion of therapeutic options? European journal of clinical investigation 2009, **39**: 81-93.

11- Martínez B.B., Pereira A.C., Muzetti J.H., Telles F.P., Mundim F.G., and Teixeira M.A. : Experimental model of glucocorticoid-induced insulin resistance. Acta Cir. Bras 2016., **31(10):** 645-9.

12- Duncan B.B., Schmidt M.I., Pankow J.S., Ballantyne, C.M., Couper D., Vigo A., et al. : Atherosclerosis Risk in Communities Study. Low-grade systemic inflammation and the development of type 2 diabetes. Diabetes 2003, **52:** 1799–805.

13- Petersen K.F., Dufour S., Befroy D., Garcia R., and Shulman G.I. : Impaired mitochondrial activity in the insulin-resistant offspring of patients with type 2 diabetes. N. Engl. J. Med. 2004 , **350:** 664–71.

14- Luc K., Schramm-Luc A., Guzik T.J., and Mikolajczyk T.P: Oxidative stress and inflammatory markers in prediabetes and diabetes. J Physiol Pharmacol 2019,**70** (6)

15- Jakubiak G.K., Osadnik K., Lejawa M., Osanik T., Golawski M., Lewandowski P., et al. :"Obesity and insulin resistance" is the component of the metabolic syndrome most strongly associated with stress. Antioxidants 2022, **11:** P79.

16- Gonzalez-Gonzalez J. G., Mireles-Zavala L. G., Rodriguez-Gutierrez R., Gomez-Almaguer D., Lavalle-Gonzalez F. J., Tamez-Perez H. E., et al. ;Hyperglycemia related to high-dose glucocorticoid use in noncritically ill patients. Diabetol. Metab. Syndr 2019., **4:** 5:18.

17- Dasgeb B., Kornreich D., McGuinn K., Okon L., Brownell I. and Sackett D. L.: Colchicine: an ancient drug with novel applications. British Journal of Dermatology 2018 , **178(2):**350–6

18- Thompson P. L. (2019): Colchicine in Cardiovascular Disease: Repurposing an Ancient Gout Drug. Clinical Therapeutics, **41(1):** 8–10

19- Gasparyan A.Y., Ayvazyan L., Yessirkepov M., and Kitas G.D. : Colchicine as an anti-inflammatory and cardioprotective agent. Expert. Opin. Drug Metab. Toxicol 2015, **11:** 1781–94.

20- Nidorf S.M., Fiolet A.T.L., Mosterd A., Eikelboom J.W., Schut A., Opstal T.S.J., et al. : Colchicine in patients with chronic coronary disease. N. Engl. J. Med. 2020, **383(19):** 1838–47.

21- Sahin M., Uguz A.C., Demirkan H., and Naziroglu M. : Colchicine modulates oxidative stress in serum and leucocytes from remission patients with family Mediterranean fever through regulation of Ca^{2+} release and the antioxidant system. J. Membrane Biol 2011., **240:** 55–62.

22- Demidowich A.P., Levine J.A., Onyekaba G.I., Khan S.M., Chen K.Y., Brady S.M., et al. : Effects of colchicine in adults with metabolic syndrome: A pilot randomized controlled trial. Diabetes. Obes. Metab. 2019, **21:**1642–51.

23- Zălar D.M., Pop C., Buzdugan E., Kiss B., Stefan M.G., Ghibu S., et al. : Effects of colchicine in a rat model of diet-induced hyperlipidemia. Antioxidants 2022, **11:** P230.

24- Zhang D., Li L., Li J., Wei Y., Tang J., Man X., Liu F.: Colchicine improves severe acute pancreatitis-induced acute lung injury by suppressing inflammation, apoptosis and oxidative stress in rats. Biomed 2022 . Pharmacother., **153:** 113461.

25- Sorg D.A., and Buckner B.): A SIMPLE METHOD OF OBTAINING VENOUS BLOOD FROM SMALL LABORATORY ANIMALS. Proc Soc Exp Biol Med 1964 1, 115:1131-2.

26- Sun G, Bishop J, Khalili S, Vasdev S, Gill V, Pace D, et al. : Serum visfatin concentrations are positively correlated with serum triacylglycerols and down-regulated by overfeeding in healthy young men. Am J Clin Nutr 2007, ***85(2):*** 399-404.

27- Matthews D.R., Hosker J.P., Rudenski A.S., Naylor B.A., Treacher D.F., and Turner R.C. : Homeostasis model assessment: insulin resistance and beta-cell function from fasting plasma glucose and insulin concentrations in man. Diabetologia 1985, **28(7):**412-9.

28-layton C., and Bancroft J. D: Carbohydrates. In K. S. Suvarna, C. Layton, & J. D. Bancroft (Eds.), Bancroft's Theory and Practice of Histological Techniques E-Book 2018 (8 ed., pp. 176-197): Elsevier Health Sciences.

29- Kiernan J. : Histological and Histochemical Methods: Theory and practice 2015 (5th ed., pp. 184-205, 455-490): Scion Publishing.

30- Kleiner D. E., Brunt E. M., Van Natta M., Behling C., Contos M. J., Cummings O. W., et al. : Design and validation of a histological scoring system for nonalcoholic fatty liver disease. Hepatology 2005, **41(6)**: 1313-21

31- Bedossa P. : Histological Assessment of NAFLD. *Digestive Diseases and Sciences 2016,* **61(5):** 1348-55.

32- Coutinho A.E., and Chapman K.E. : The anti-inflammatory and immunosuppressive effects of glucocorticoids, recent developments and mechanistic insights. Mol. Cell Endocrinol 2011, **335:** 2–13.

33- Barel M., Perez O.A.B., Giozzet V.A., Rafacho A., Bosqueiro J.R., do Amaral S.L. : Exercise training prevents hyperinsulinemia, muscular glycogen loss and muscle atrophy induced by dexamethasone treatment. *Eur. J. Appl. Physiol 2010.*, **108:** 999–1007.

34- Shpilberg Y., Beaudry J.L., D'Souza A., Campbell J.E., Peckett A., Riddell M.C. : A rodent model of rapid-onset diabetes induced by glucocorticoids and high-fat feeding. *Dis Model Mech 2012.*, **5(5):** 671-80.

35- Arab Dolatabadi A., and Mahboubi M. : A study of the influence of dexamethasone on lipid profile and enzyme lactate dehydrogenase. *J. Med. Life*, **8(3):** 72-6.

36- Feng X., Zhao Y., Yang T., Song M., Wang C., Yao Y., Fan H.): Glucocorticoid-Driven NLRP3 Inflammasome Activation in Hippocampal Microglia Mediates Chronic Stress-Induced Depressive-Like Behaviors. *Front Mol Neurosci 2019*, **29(**12):210.

37- Wang L., Jiao X.F., Wu C., Li X.Q., Sun H.X., Shen X.Y., et al. : Trimetazidine attenuates dexamethasone-induced muscle atrophy via inhibiting NLRP3/GSDMD pathway-mediated pyroptosis. *Cell Death Discov 2021.*, **7(1):** 251.

38- Zhang X., Pang R., Zhang K., Xu Q., Xu C., Shi W., et al. : Apocynin exerts cytoprotective effects on dexamethasone-induced osteoblasts by inhibiting oxidative stress through the Nrf2 signalling pathway. *J. Cell Mol. Med2023.*, **27(23):** 3911-27.

39- Bartram U., and Speer C.P.,): The role of transforming growth factor beta in lung development and disease. *Chest 2004.*, **125:** 754–65.

40- Feng X.L., Fei H.Z, and Hu L. : Dexamethasone induced apoptosis of A549 cells via the TGF-β1/Smad2 pathway. *Oncol. Lett 2018.*, **15:** 2801-6.

41- Shi K., Jiang J., Ma T., Xie J., Duan L., Chen R., et al. : Dexamethasone attenuates bleomycin-induced lung fibrosis in mice through TGF-β, Smad3 and JAK-STAT pathway. Int. J. Clin. Exp. Med 2014., **7(9):** 2645-50.

42- Ghosal S., Duman C.H., Liu R.J., Wu M., Terwilliger R., Girgenti M.J., et al. : Ketamine rapidly reverses stress-induced impairments in GABAergic transmission in the prefrontal cortex in male rodents. *Neurobiol. Dis 2020*, ***134*:** 104669.

43- Alhaddad A., Radwan A., Mohamed N.A., Mehanna E.T., Mostafa Y.M., El-Sayed N.M., et al. : Rosiglitazone Mitigates Dexamethasone-Induced Depression in Mice via Modulating Brain Glucose Metabolism and AMPK/mTOR Signaling Pathway. *Biomedicines 2023*, **11(3):** 860.

44- Kurt R.K., Dogan A.C., Dogan M., Albayrak A., Kurt S.N., Eren F., et al. : Protective Effect of Colchicine on Ovarian Ischemia—Reperfusion Injury. Reproductive Sc 2015i., **22(5):** 545-50.

45- Wang Y., Viollet B., Terkeltaub R., and Liu-Bryan R. : AMP- activated protein kinase suppresses urate crystal- induced inflammation and transduces colchicine effects in macrophages. Ann. Rheum. Dis. 2016, **75:** 286–94.

46- Wang L., Sawhney M., Zhao Y., Carpio G.R., Fonseca V., and Shi L. : Association between colchicine and risk of diabetes among the veterans affairs population with gout. Clin. Ther 2015., **37:** 1206–15.

47- Robertson S., Martínez G. J., Payet C. A., Barraclough J. Y., Celermajer D. S., Bursill C., et al. : Colchicine therapy in acute coronary syndrome patients acts on caspase-1 to suppress NLRP3 inflammasome monocyte activation. Clin. Sci. (Lond)., **130(14):** 1237–46.

48- Shen S., Duan J., Hu J., Qi Y., Kang L., Wang K., et al. : Colchicine alleviates inflammation and improves diastolic dysfunction in heart failure rats with preserved ejection fraction.European Journal of Pharmacology 2022, **929** 175126,ISSN 0014-2999.

49- Leung, Y.Y.; Yao Hui, L.L.; Kraus, V.B. : Colchicine— update on mechanisms of action and therapeutic uses. Semin Arthritis Rheum. 2015, **45:** 341–50.

50- Ridker P.M., and Lüscher T.F. : Anti-inflammatory therapies for cardiovascular disease. Eur Heart J 2014, **35(27):**1782-91.

51- Esser N., L'Homme L., De Roover A. Kohnen L., Scheen A.J., Moutschen M., et al. : Obesity phenotype is related to NLRP3 inflammasome activity and immunological profile of visceral adipose tissue. Diabetologia 2013, **56:** 2487–97.

52- Jourdan T., Godlewski G., Cinar R., Bertola A., Szanda G., Liu J., et al. : Activation of the Nlrp3 inflammasome in infiltrating macrophages by endocannabinoids mediates beta cell loss in type 2 diabetes. Nat. Med. 2013, **19(9):** 1132–40.

53- Vandanmagsar B., Youm Y.H., Ravussin A., Galgani J.E., Stadler K., Mynatt R.L., et al.): The NLRP3 inflammasome instigates obesity-induced inflammation and insulin resistance. Nat Med 2011, **17(2):**179-88.

54- Khan R., and Sheppard R. : Fibrosis in heart disease: understanding the role of transforming

growth factor-beta in cardiomyopathy, valvular disease, and arrhythmia. Immunology 2006, **118(1):**10–24.

55- Ross S., Cheung E., Petrakis T.G., Howell M., Kraus W.L., and Hill C.S. : Smads orchestrate specific histone modifications and chromatin remodeling to activate transcription. EMBO J 2006., **25(19):** 4490–502.

56- Simonsson M., Kanduri M., Gronroos E., Heldin C.H., and Ericsson J. : The DNA binding activities of Smad2 and Smad3 are regulated by coactivator-mediated acetylation. J. Biol. Chem. 2006, **281(52):** 39870–80.

57- Suryono S., Rohman M.S., Widjajanto E., Prayitnaningsih S., Wihastuti T.A., Oktaviono Y.H. : Effect of Colchicine in reducing MMP-9, NOX2, and TGF- β1 after myocardial infarction. BMC Cardiovasc. Disord 2023., 23(1): 449.

58- Xu S., Cai Y., Wei Y. : mTOR Signaling from Cellular Senescence to Organismal Aging. *Aging Dis 2014.*, **5**(4): 263–73.

59- Zhou H., Khan D., Hussain S.M., Gerdes N., Hagenbeck C., Rana M., et al. : Colchicine prevents oxidative stress-induced endothelial cell senescence via blocking NF-κB and MAPKs: implications in vascular diseases. *J. Inflamm2023.*, **20(1):** 41.

60- Dai C., Brissova M., Reinert R. B., Nyman L., Liu E. H., Thompson C., et al. : Pancreatic Islet Vasculature Adapts to Insulin Resistance Through Dilation and Not Angiogenesis. *Diabetes2013* , **62(12):** 4144-53.

61- Rafacho A., Cestari T. M., Taboga S. R., Boschero A. C., and Bosqueiro J. R. : High doses of dexamethasone induce increased beta-cell proliferation in pancreatic rat islets. *Am J Physiol Endocrinol Metab 2009*, ***296*(4):** 681-9.

62- Hirsova P., and Gores G. J. : Ballooned hepatocytes, undead cells, sonic hedgehog, and vitamin E: therapeutic implications for nonalcoholic steatohepatitis. *Hepatology 2015*, ***61*(1)**: 15-17.

63- Machado M. V., and Diehl A. M. : Pathogenesis of Nonalcoholic Steatohepatitis. *Gastroenterology 2016* , ***150*(8):**1769-77.

64- Li Y.Y., Zheng T.L., Xiao S.Y., Wang P., Yang W.J., Jiang L.L., et al.. : Hepatocytic ballooning in non-alcoholic steatohepatitis: Dilemmas and future directions. Liver Internationa 2023l, **43(6)**: 1170-82.

65- Lackner C., Gogg-Kamerer M., Zatloukal K., Stumptner C., Brunt E. M., and Denk H. : Ballooned hepatocytes in steatohepatitis: The value of keratin immunohistochemistry for diagnosis. Journal of Hepatology 2008 , **48(5)**: 821-8.

66- Younossi Z. M., Stepanova M., Rafiq N., Henry L., Loomba R., Makhlouf H., et al. : Nonalcoholic steatofibrosis independently predicts mortality in nonalcoholic fatty liver disease. *Hepatol Commun*, *2017* ***1*(5):** 421-8.

67- Kakisaka K., Cazanave S. C., Werneburg N. W., Razumilava N., Mertens J. C., Bronk S.F., et al.): A hedgehog survival pathway in 'undead' lipotoxic hepatocytes. *Journal of Hepatology2012* , ***57(4):*** 844-51.

68- Kakisaka K., Suzuki Y., Fujiwara Y., Abe T., Yonezawa M., Kuroda H.,et al. (2018): Evaluation of ballooned hepatocytes as a risk factor for future progression of fibrosis in patients with non-alcoholic fatty liver disease. Journal of Gastroenterology 2018, 53(12): 1285-1291. doi:10.1007/s00535-018-1468-9

69- Rafiq N., Bai C., Fang Y., Srishord M., McCullough A., Gramlich T., et al. : Long-term follow-up of patients with nonalcoholic fatty liver. *Clin Gastroenterol Hepato 2009l*, ***7*(2):** 234-8.

70- Dixon L. J., Berk M., Thapaliya S., Papouchado B. G., and Feldstein A. E. : Caspase-1-mediated regulation of fibrogenesis in diet-induced steatohepatitis. *Laboratory Investigation 2012*, **92(5):** 713-23.

71- Abdul-Hay S. O., Kang D., McBride M., Li L., Zhao J., and Leissring M. A. : Deletion of Insulin-Degrading Enzyme Elicits Antipodal, Age-Dependent Effects on Glucose and Insulin Tolerance. *PloS one 2011*, **6(6):** 20818.

Citation

Nageeb, M., Mortada Mahmoud, S., Ali Mohamed Ali, S., Hendy, N., M. Ahmad, M., A. Hemead, D. Colchicine alleviates steroid-induced Hyperglycemia and Dyslipidemia: Targeting Pyroptosis and Oxidative stress. *Zagazig University Medical Journal*, 2025; (695-713): -. doi: 10.21608/zumj.2024.333297.3674